ALLOY DESIGN FOR UOE LINEPIPE MATERIAL FOR STANDARD AND NON-STANDARD HIC CONDITIONS

C. Stallybrass, T. Haase, J. Konrad, C. Bosch and A. Kulgemeyer

Salzgitter Mannesmann Forschung GmbH
Ehinger Straße 200, 47259 Duisburg, Germany

Keywords: Alloy Design, NACE, Low Alloy Steel, HIC, Sour Service, H_2S, Fit-for-Purpose, Composition, Large Diameter Pipe, Linepipe, X65, X70, Segregation

Abstract

The last several decades have seen a steady increase in the demand for high-strength linepipe steels. These offer the most economical option to transport large gas volumes at high pressures from remote areas to the market. Since the beginning of the 1980s, Salzgitter Mannesmann has been involved in the development of high strength heavy plates. Since then, these products have steadily been improved, for example in terms of toughness and weldability. As gas resources in increasingly hostile environments are developed, the requirements with regard to mechanical properties gain growing significance. A similar market trend towards higher strength levels is currently evident in the field of HIC-resistant pipe materials.

The transport of natural gas, containing hydrogen sulphide, leads potentially to hydrogen uptake in the material which can cause damage via two distinct mechanisms. Hydrogen induced cracking (HIC) takes place without any external stress, while sulphide stress cracking (SSC) occurs in the presence of a critical tensile stress. Even though both mechanisms involve dissolved hydrogen, they are not directly connected. The present paper reviews the restrictions on the alloy design and the production processes that have to be taken into account in order to produce HIC-resistant large-diameter pipe material. Because of these restrictions, the production of HIC-resistant pipes has been largely limited to API Grades up to X65 for standard conditions, according to NACE TM0284. Investigations of the limits of HIC-resistance have been carried out at Salzgitter Mannesmann Forschung, using pipe material beyond the X65 strength level, in order to evaluate the potential of these materials for use under fit-for-purpose[1] test conditions, ie. at higher pH-levels and lower H_2S partial pressures. The test results have been compared to SSC severity regions according to ISO 15156-2 for the investigated materials.

Introduction

Pipelines used for the transport of media containing wet hydrogen sulphide (H_2S) are faced with the danger of sudden and severe cracking. In sour environments containing water and H_2S, hydrogen atoms that originate from the anodic dissolution of the material may diffuse into the steel. This can lead to different forms of cracking, such as hydrogen induced cracking (HIC), sulphide stress cracking (SSC) or stress oriented hydrogen induced cracking (SOHIC) [1,2]. The presence of liquid water, necessary for initiation of these mechanisms, can result even when the gas temperature in the pipeline is above the water dew point, if the water vapour condenses on the colder pipe walls. Due to the sudden and unforeseeable appearance

[1] This term is used as defined in ISO 15156-2.

of these failure mechanisms, it is necessary to use HIC resistant pipeline steel for application under sour service conditions.

In the case of HIC, the stress is generated internally by the pressure of gaseous molecular hydrogen through hydrogen recombination at impurities (inclusions), imperfections or microstructural irregularities [3-5]. This leads to step-wise cracks that are typically parallel to the rolling plane. SSC, on the other hand, is primarily a surface phenomenon that requires external and/or residual stresses and leads to transgranular cracks that are perpendicular to the surface of the sample. In order to obtain resistance against HIC, factors that contribute to the initiation and propagation of cracks have to be minimized. Inclusions that originate, either from steelmaking, or as a consequence of solidification, are likely sites for HIC initiation. Crack propagation is facilitated by microstructural inhomogeneities resulting from segregation and can be influenced to some extent by the alloy design and production parameters.

The standardized laboratory test, according to NACE TM 0284-2011 [6] or EFC 16 [7], for the determination of HIC resistance provides a relative measure of the cracking susceptibility of material which is established under severely sour test conditions. The material is qualified for the intended application when the test is successfully passed. The test is not intended to reproduce service conditions, but to provide reproducible test environments to determine the relative HIC susceptibility under very severe conditions within a short time. Material which fails the test may still be fit-for-purpose in field environments that are normally less severe than the standardized test solution. There is a strong market interest to use linepipe grades above the X65 strength level to allow higher operating pressures. Efforts are therefore being made worldwide to adapt the HIC test method for fit-for-purpose (FFP) evaluations, taking into account the actual service conditions.

ISO 15156-2 [8] provides an FFP approach for SSC-testing by defining sour service conditions of different severity. The SSC regions cannot be applied directly to HIC testing due to the different failure modes of the two corrosion mechanisms. In order to provide a similar approach for HIC, the severity regions have to be redefined. Within this paper, results of HIC tests using large diameter X65 and X70 pipe material are presented, in which the pH-level and the H_2S partial pressure were varied systematically, in order to establish the limits for sour service applications.

Alloy Design

It has been shown that HIC resistance depends both on reduction of the initiation sites and on the reduction of factors that contribute to the propagation of hydrogen-induced cracks [9]. Oxide inclusions have been associated with HIC initiation and strategies have been developed to minimize their effect by improved steelmaking and continuous casting technology [10,11]. The positive effect of preventing the formation of elongated MnS inclusions by desulphurization and inclusion shape-control via calcium-treatment [9,12] and maintaining low phosphorus-levels [13] are equally well documented. However, tight control of these processing steps alone is not sufficient to guarantee HIC resistance, especially when targeting strength levels above X65. Alloy designs play an important role when developing sour service steels. In the following sections, the effects of the alloy design on factors that contribute to HIC, along the processing steps from solidification to rolling, are illustrated.

During continuous casting the solidification of steel is a process that may lead to an inhomogeneous distribution of alloying elements. This in turn affects the microstructure of the final product. Segregation can be observed on two different length scales. As the strand shell solidifies, dendrites begin to grow towards the liquid core of the strand. The volume fraction of the liquid between the dendrites decreases with decreasing temperature and elements that have a low solubility in the solid phase accumulate there, particularly if the solute diffusivity is low, restricting their redistribution.

The degree of the variation in composition at the scale of the solidified dendrite arms is micro-segregation. As such, although it can be quite severe in terms of the absolute degree of segregation, it is usually of only minor impact owing to its small scale with compositional variations occurring over a scale of approximately 100 microns. However, mechanical and thermo-solutal effects in the semi-solid mushy-zone can lead to some of this micro-segregate moving through the mushy zone and gathering in larger volumes, for example, along the centerline, which is termed macro segregation and which can be more problematic in terms of its effect on material properties.

Since diffusion is significantly faster in the body-centred cubic lattice of the delta ferrite (δ) than in the face-centred cubic lattice of the austenite (γ), it follows that a large stability range of delta ferrite facilitates the redistribution of elements in the solid phase. As illustrated in the Fe-C equilibrium phase diagram in Figure 1, the stability range of delta ferrite increases with decreasing carbon content.

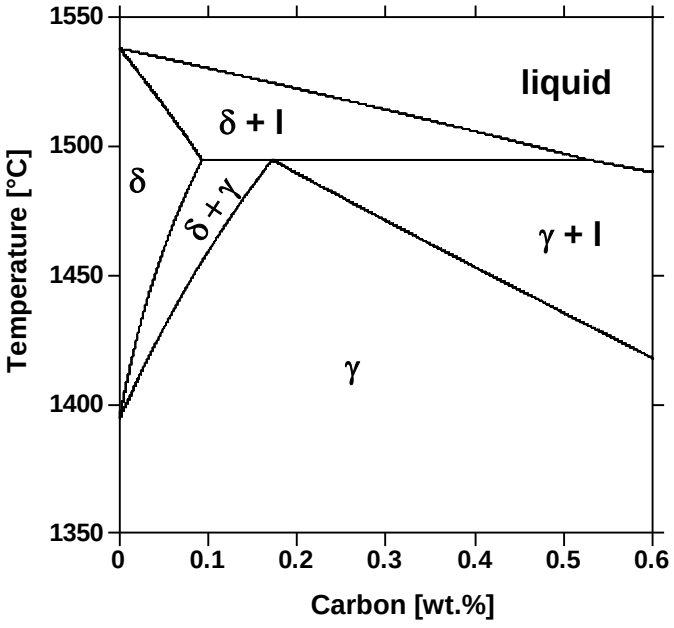

(a)

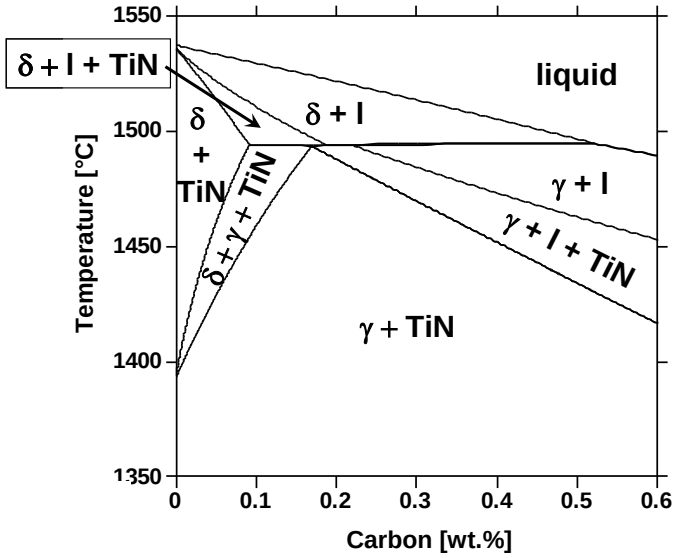

Figure 1. Phase diagram of Fe-C (a) and Fe-0.025%Ti-0.005%N-C isopleth (b) between 1350 °C and 1550 °C calculated with Thermo-Calc in combination with the TCFE5 database, adapted from [14].

If the solubility of an element in the solid phase is low, this element will be enriched in the liquid phase. This enrichment can reach such high levels that other primary phases can form before solidification is completed. As an example, the primary formation of TiN is given in the Fe-0.025 %Ti-0.005 %N-C isopleths in Figure 1 [14]. Such high temperature primary precipitates can have a detrimental influence on HIC resistance, since the TiN precipitates will also act as initiation sites if they reach a critical size.

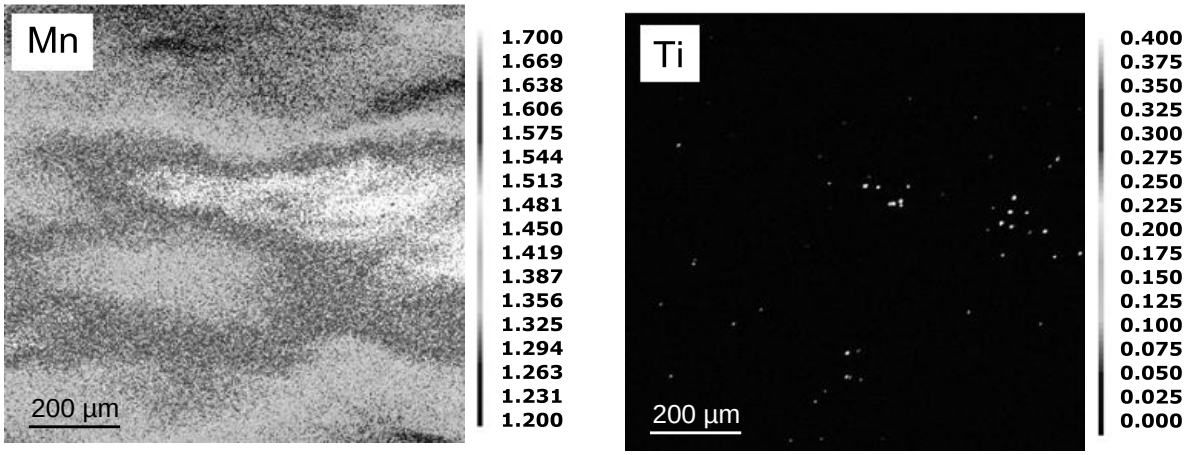

Figure 2. Variation of the manganese and titanium content (wt.%) within the centerline segregation of X65 heavy plate material as measured by EPMA at a step size of 2 µm [14].

Experimental evidence of the primary precipitation of TiN is shown in Figure 2 in an electron probe microanalysis (EPMA) mapping of the distribution of manganese and titanium in X65 heavy plate material in the vicinity of the centerline. Through similar partitioning mechanisms many other elements can also segregate [15,18]. Clearly, therefore, minimizing centerline segregation is an essential preliminary step in developing sour service linepipe steels. Progress in this direction has been made in recent years by the introduction of

improved tundish and continuous casting practices but it is the drive towards significantly reduced carbon levels which holds the key to the effective elimination of this problem.

Experimental investigations have shown that a reduced carbon content leads to lower enrichment of manganese, both in the microsegregated regions, as well as at the centerline [16,17]. The beneficial effect on microsegregation can be attributed to the redistribution of manganese within the larger delta-ferrite range at low carbon levels. The effect of the carbon content on the ratio of the maximum and nominal manganese content within the centerline was investigated using EPMA measurements and is illustrated in Figure 3. This plot demonstrates that a ratio of 1.5 can be maintained at a carbon content of below 0.04%. A further reduction in carbon does not lead to further improvement and may lead to reduced strength levels. An increase in the carbon content above 0.05%, on the other hand, would have to be counterbalanced by a reduction in manganese content in order to achieve the same manganese level in the centerline segregation band.

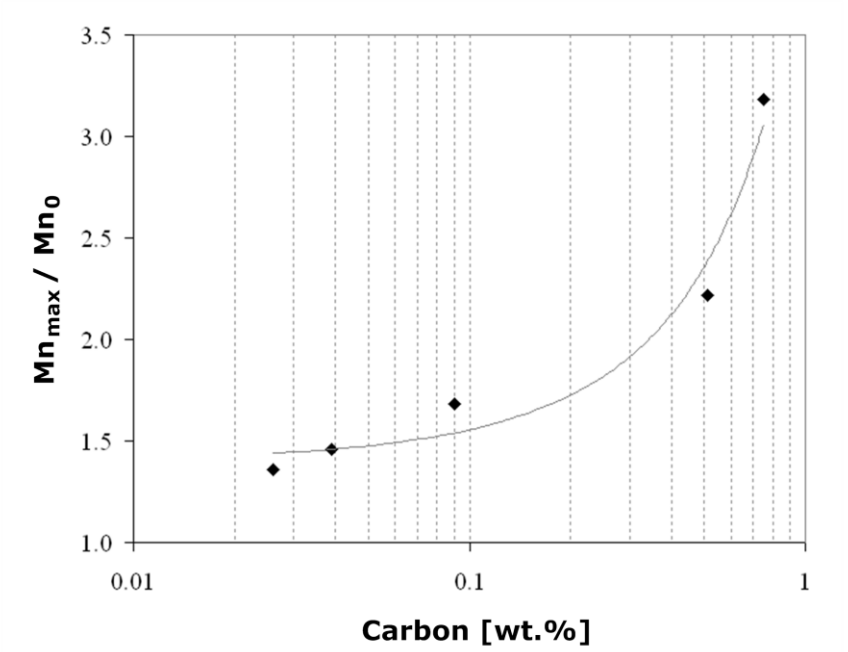

Figure 3. Correlation of the carbon content with manganese enrichment in the centerline segregation region of low alloy steels, adapted from [8].

A similar trend was observed by spark-emission spectroscopy of slab material, not intended for sour service, that was measured at different distances from the centerline [15,17], as shown in Figure 4. The composition of this steel is shown in Table I below.

Table I. Chemical Composition of Steel Investigated, wt.%

C	Mn	Si	S	P	Al	Cu	V	Nb
0.066	1.26	0.26	0.001	0.011	0.02	0.29	0.04	0.03

Because the results in Figure 4 are integral values of the analysed volume in a sample, which is several mm in diameter and roughly 0.1 mm in thickness, the peak values are naturally lower than they would be in the case of EPMA measurements, where the analysed volume has a diameter of only several μm. The plots show a significant enrichment of carbon,

manganese and phosphorus at the centerline. The enrichment in carbon and manganese observed by spark emission spectroscopy and EPMA measurements at the centerline, are significant but as proven elsewhere, a reduction in the carbon content to below 0.04% was found to lead to a significant reduction in centreline segregation [15].

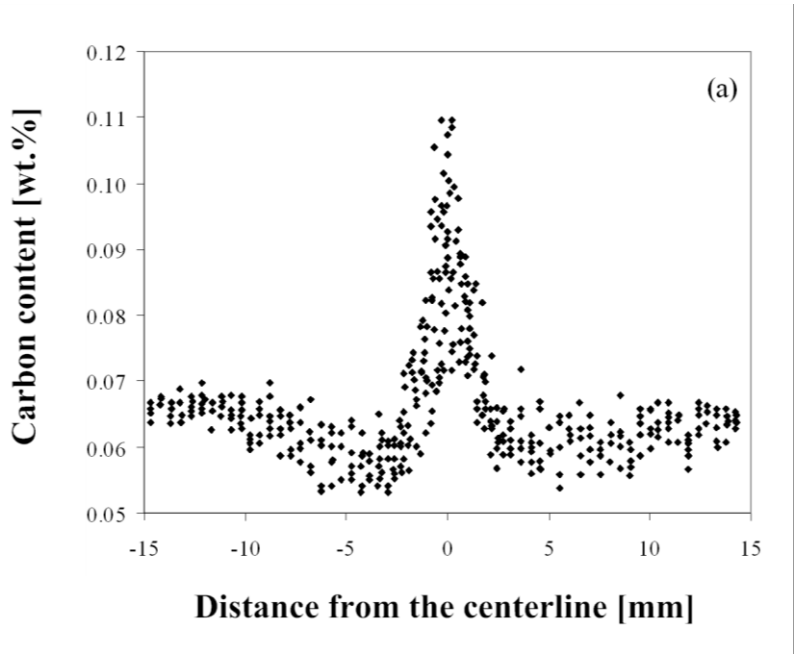

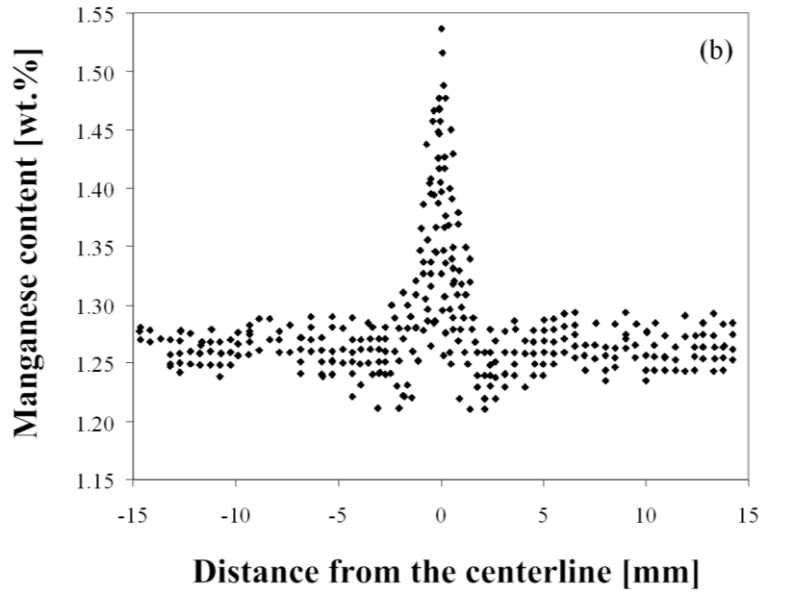

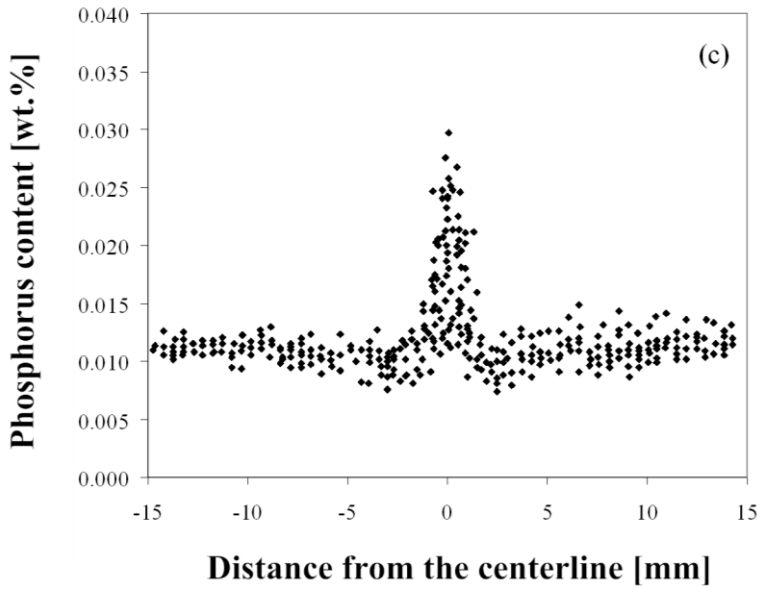

Figure 4. Distribution of carbon (a), manganese (b), phosphorus (c) in the vicinity of the centerline of continuous cast material as measured by spark emission spectroscopy, adapted from [15,17].

Modern thermodynamic modelling tools are capable of describing the formation of the microsegregation for a given composition and cooling conditions. As an example, the enrichment of manganese in a dendrite and the interdendritic liquid at an early stage of solidification of a low-alloy steel obtained by Phase Field simulation is shown in Figure 5. Prediction of the macrosegregation based on a physical model is unfortunately more complex, as the formation and morphology depends strongly on the continuous casting conditions. However, progress in this field of modelling is promising.

Figure 5. Manganese distribution (wt.%) within dendrites (top) and the liquid phase (bottom) obtained by Phase Field simulation of the solidification of a low-alloy steel.

Thermomechanical rolling is the next step in the production of heavy plates for linepipe. Reheating of the slab material aims at achieving a homogeneous distribution of microalloying elements so that carbonitride precipitates can form during rolling. Thermodynamic modelling can be used for the selection of appropriate reheating temperatures. The result of an equilibrium calculation is shown in Figure 6 for the VNb-microalloyed model composition shown in Table II. In this case, NbC is dissolved at around 1020 °C.

Table II. Chemical Composition, wt.%

C	Si	Mn	Al
0.04	0.3	1.4	0.03

While the aim of reheating is to dissolve niobium carbide, excessively high temperatures have to be avoided in order to prevent grain growth of the austenite, which can have a detrimental effect on mechanical properties.

During thermomechanical rolling, the niobium carbide precipitates retard recrystallisation significantly in the temperature range, typically below 950 °C. Deformation in this range, therefore, leads to elongation of austenite grains (pancaking) and strengthening of the austenite grains and a high density of nucleation sites for the γ–α phase transformation that takes place during cooling. The result is a grain size typically below 10 μm and an excellent combination of strength and low-temperature toughness. Air cooling of the plate typically results in a ferritic-pearlitic microstructure while accelerated cooling leads to a predominantly bainitic microstructure and even smaller effective grain sizes.

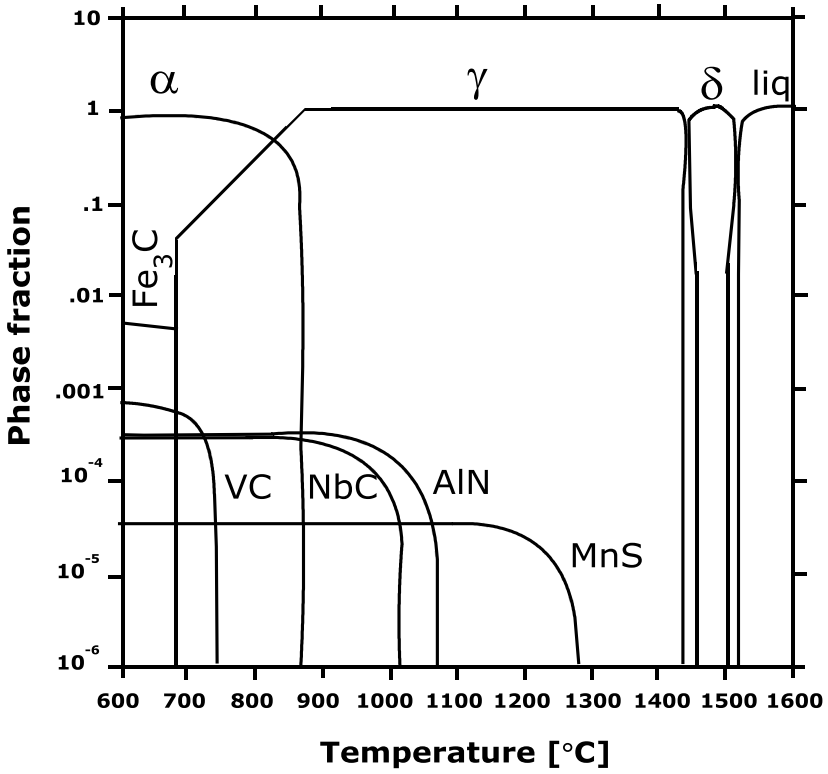

Figure 6. Phase fraction as a function of temperature for a model composition calculated with Thermo-Calc in combination with the TCFE5 database.

Since the solubility of carbon in ferrite is about two orders of magnitude lower than in the austenite, the carbon is continuously redistributed to the austenite in the $\gamma+\alpha$ temperature range during air cooling, facilitated by its rapid interstitial diffusion. Any remaining microsegregation of the substitutional elements from the casting process will include local enrichment of manganese, which in turn lowers the transformation temperature (Ar_3) in these enriched regions, ie. the pearlite islands, which are the regions where the austenite transformed last, correlate with areas of increased manganese content. This is even more pronounced at the plate centerline where the enrichment of manganese is greatest. If the centerline segregation is strongly pronounced, this can lead to the formation of a bainitic or martensitic microstructure with increased hardness at the centerline which can facilitate HIC propagation. A low carbon content, below 0.05%, contributes to a homogeneous microstructure in the plate material after air cooling by lowering the volume fraction of pearlite and reducing the severity of centerline segregation.

Accelerated cooling, on the other hand, leaves less time for carbon redistribution during the phase transformation which has a positive effect on the homogeneity of the microstructure. The beneficial effect this exerts on HIC behavior has been reported by Tamehiro et al [18]. It was found that accelerated cooling should start above Ar_3 and that cooling rates above 15 K/s should be used for best results. Using this strategy, good HIC resistance was achieved with material that failed if air cooling was applied. This suggests that the restrictions regarding carbon and manganese can be loosened if accelerated cooling is used in heavy plate production.

Fit-for-Purpose Testing

Standard HIC-testing, according to NACE TM0284-2011, is typically performed using pure hydrogen sulphide gas of high quality. For HIC-testing under fit-for-purpose conditions at a fixed H_2S partial pressure, represented by a gas mixture of H_2S in N_2 or CO_2, bottled or pre-mixed test gas can be purchased in the same manner as pure H_2S. This has the drawback that the test laboratory has to order test gas from a commercial distributor with the desired composition well in advance, as delivery times can be several weeks due to the long gas mixing process. Bottled pre-mixed gas has an expiry date beyond which it cannot be used. Limitations in storage capacity and safety issues can complicate matters even further. In addition, different gas mixtures are required for each testing condition.

In order to overcome these difficulties, a method for in-situ gas mixing of pure gases, during the test, was developed at Salzgitter Mannesmann Forschung GmbH [19]. This requires the controlled flow of gas independent of the background and outlet pressure and temperature. It was found that this is possible using commercially available mass-flow controller units. The in-situ gas mixing setup, shown in Figure 7, consists of two mass flow controllers and a turbulent mixing zone above the test vessel. This setup makes it possible to use H_2S partial pressures up to 0.5 bar in N_2 or CO_2 and the correct operation of the equipment has been validated by frequent measurement of the H_2S concentration in the test solution. This method increases the flexibility to assess the HIC-resistance of a given material under a variety of conditions. In the following paragraphs, an example is given of a test series that was performed with this setup using material prone to HIC.

Figure 7. In-situ test gas mixing system connected to test vessel.

HIC-tests were performed, according to NACE TM0284-2011, on standard specimens taken from a pipe with an outer diameter of 914 mm and a wall thickness of 43.2 mm, produced using HIC-susceptible X70 steel. The chemical composition of this material designed for non-sour application is shown in Table III.

Table III. Chemical Composition, wt.%

C	Si	Mn	P	S	Nb	Others
0.05	0.3	1.55	<0.02	<0.002	0.04	Cu, Ni, V, Ti

Based on the arguments presented above, it is certain that this material is prone to HIC because of its chemical composition. In addition, the steel was produced under standard non-sour conditions.

The test conditions ranged from a H_2S partial pressure of 0.02 bar to 0.1 bar in CO_2 and NACE TM0284-2011 standard conditions of 1 bar H_2S at a start pH of 2.7. Both the test solution recommended in EFC 16, Annex A, and NACE TM0284 Solution A were used. The specimens were evaluated by ultrasonic inspection and in selected cases by metallography. Figure 8 shows the crack area ratio (CAR) that was found for the individual testing conditions. This diagram shows that the material is cracking resistant up to a partial pressure of H_2S of nearly 0.1 bar.

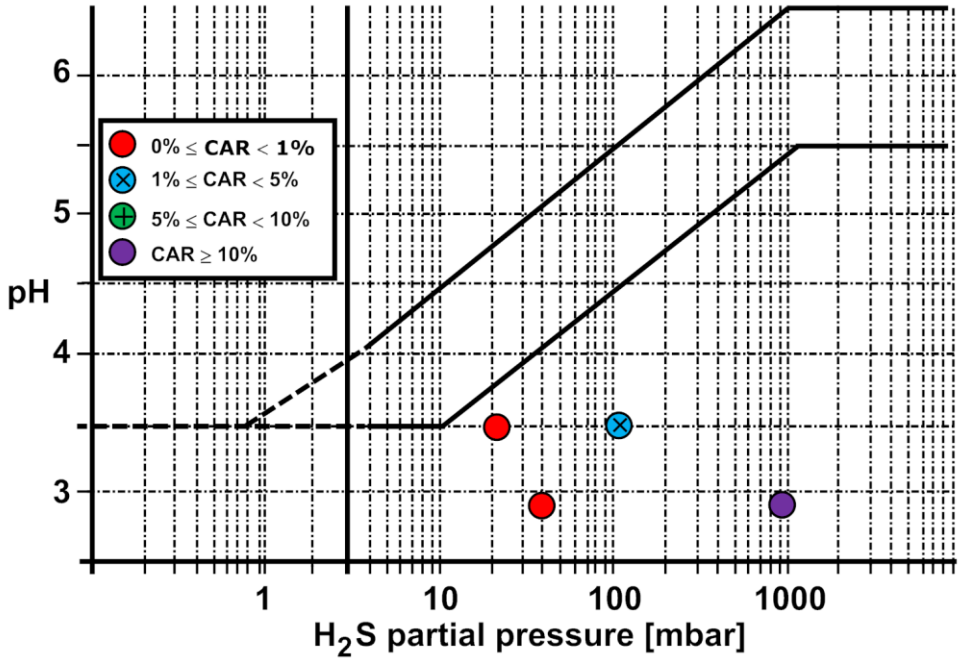

Figure 8. HIC severity matrix for X70 non-sour base metal compared to SSC severity regions.

Results of a similar investigation using HIC-susceptible X65 material taken from a pipe with an outer diameter of 1016 mm and a wall thickness of 22.23 mm are given in Figure 9 [20]. In this investigation, pre-mixed bottled gas was used with different partial pressures of H_2S in CO_2. The steel composition is shown in Table IV.

Table IV. Chemical Composition, wt.%

C	Si	Mn	P	S	Nb+V+Ti
0.09	0.3	1.58	<0.02	<0.002	0.06

The material showed HIC-resistance nearly up to a H_2S partial pressure of 0.1 bar. Ultrasonic inspection of the samples revealed that a reduction of the H_2S partial pressure from 1 bar to 0.1 bar led to a lower area fraction of HIC close to the pipe walls. However, samples that were tested at a partial pressure of 0.1 bar still showed cracks at the plate centerline, see Figure 10. This illustrates the importance of minimizing centerline segregation.

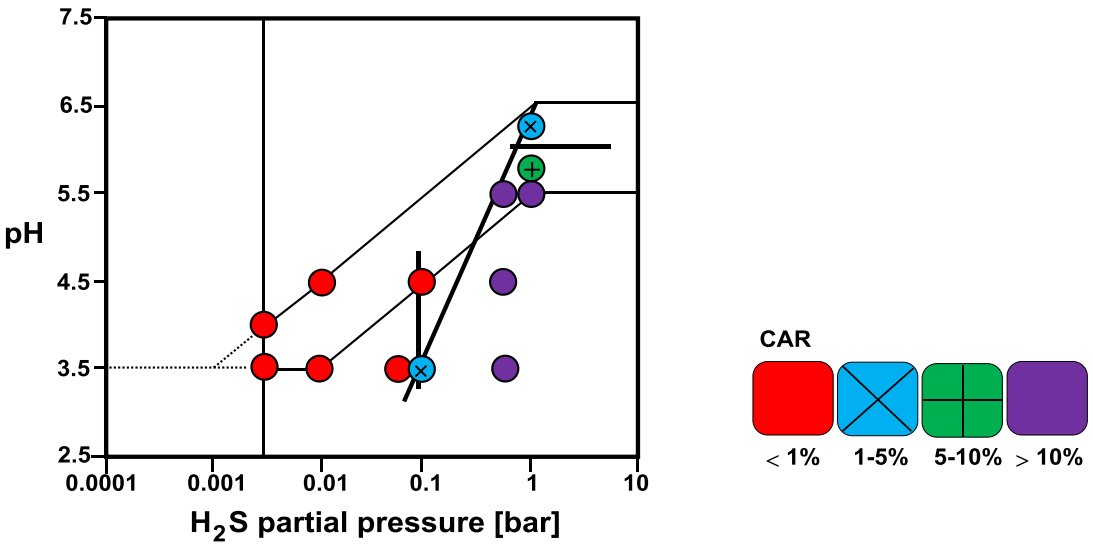

Figure 9. HIC severity matrix for X65 non-sour base metal compared to SSC severity regions.

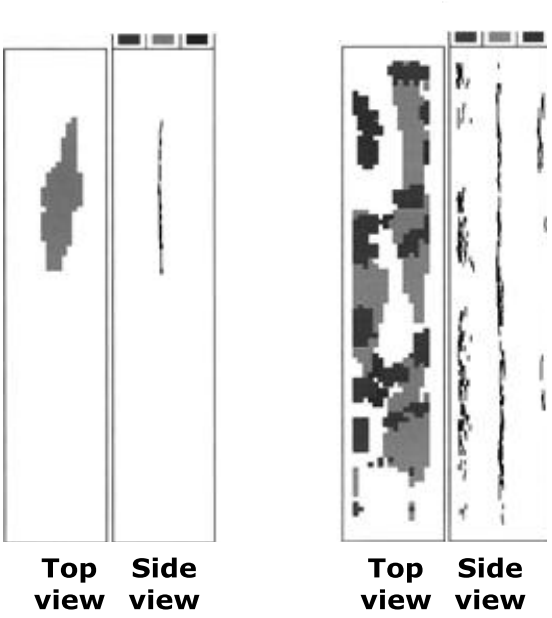

Figure 10. Typical results of ultrasonic inspection of X65 non-sour with different degrees of HIC: EFC 16-solution at 0.1 bar H_2S and pH 3.5 (left) and NACE TM0284 2011 Solution A (right) at 1 bar H_2S and pH 2.7 (start).

Conclusions

Hydrogen-induced cracking depends on factors that contribute to initiation and propagation of cracks in susceptible regions. It was shown that cleanness of the steel and inclusion shape control alone does not guarantee HIC-resistance. The established alloying concepts for HIC-resistant linepipes must be adapted for strength levels above X65. However, possibilities or desires to increase the carbon and manganese contents are limited because both strongly affect the segregation behavior. There is also a risk of the formation of primary carbonitride particles at the centerline of the strand during continuous casting. Allowable levels of microalloying elements depend on the possibilities to minimize centerline segregation. Tight control of the continuous casting parameters is, therefore, a precondition for guaranteeing HIC-resistance.

It has been shown that cooling practice has a strong effect on the homogeneity of the microstructure, which in turn influences HIC propagation. The established alloying concepts ensure that the degree of segregation is minimized so that HIC is prevented irrespective of the cooling strategy used in production. Accelerated cooling leads to a lower local inhomogeneity of the carbon distribution and has been found to have a beneficial effect on HIC-test results. This permits the use of alloying concepts that were not accessible previously for air cooling

The influence of the test conditions with regard to pH and H_2S partial pressure was presented for two HIC-susceptible materials. The results were classified into groups of different HIC-resistance in order to define HIC-severity regions similar to the SSC-regions defined in ISO 15156-2. It was found that the threshold between non-sour and slightly sour regions for HIC is shifted to higher H_2S partial pressures in both materials compared to the SSC-regions. While the materials failed the HIC-tests under standard NACE TM0284 conditions, the results showed that these materials are suitable under test regimes that simulate field conditions.

References

1. W. Dahl et al., “Untersuchungen über die Schädigung von Stählen unter Einfluß von feuchtem Schwefelwasserstoff,” *Stahl und Eisen*, 87 (1967), 125.

2. R. Pöpperling et al., “Results of Full Scale Testing and Laboratory Tests of Line Pipe Steels” (Paper presented at Corrosion 91, NACE International, Houston, TX, USA, 1991), paper 16.

3. R. Pöpperling, W. Schwenk and J. Venkateswarlu, “Arten und Formen der wasserstoffinduzierten Rißbildung an Stählen,” *VDI-Berichte,* Nr. 365 (1980), 49.

4. W. Schwenk and R. Pöpperling, “Large Pipes for Sour Gas Operations Selection of Suitable Steels, Manufacture and Test Methods,” *3R International*, 19 (1980), 571.

5. M. Iino, “The Extension of Hydrogen Blister-crack Array in Linepipe Steels,” *Metallurgical Transactions A*, 9A (11) (1978), 1581.

6. NACE TM 0284-2011, *Evaluation of Pipeline and Pressure Vessel Steels for Resistance to Hydrogen-Induced Cracking*, (Houston, TX: NACE International, 2011).

7. EFC Publication No. 16, third edition, *Guidelines on Materials Requirements for Carbon and Low Alloy Steels for H_2S Containing Environments in Oil and Gas Production,* European Federation of Corrosion (2009).

8. ISO 15156-2, *Petroleum and Natural Gas Industries – Materials for Use in H_2S Containing Environments in Oil and Gas Production – Part 2: Cracking-resistant Carbon and Low Alloy Steels and the Use of Cast Irons,* ISO (2009).

9. G. Herbsleb, R. Pöpperling and W. Schwenk, "Occurrence and Prevention of Hydrogen Induced Stepwise Cracking and Stress Corrosion Cracking of Low Alloy Pipeline Steels" (Paper presented at Corrosion 37, 1981), 247.

10. H. Jacobi and K. Wünnenberg, "Improving Oxide Cleanness on Basis of MIDAS Method" (Paper presented at Clean Steel 6, Balatonfüred/Hungary, 2002), 195.

11. A. Fuchs et al., "Bestimmung des Makroskopischen Reinheitsgrades an Strangguß-brammen durch eine Off-line-Ultraschallprüfung," *Stahl und Eisen*, 113 (1993), 51.

12. M. Iino et al., "Linepipe Resistant to Hydrogen" (Paper presented at AIME/SFM International Conference HSLA Steels – Experiences in Applications, Versailles, France, 1979).

13. I. Takeuchi et al., "Development of High Strength Line Pipe for Sour Service and Full Ring Evaluation in Sour Environment" (Paper presented at the 23rd International Conference on Offshore Mechanics and Arctic Engineering, paper number OMAE2004-51028 2004), 653.

14. A. Schneider et al., "Formation of Primary TiN Precipitates During Solidification of Microalloyed Steels – Scheil versus DICTRA simulations," *International Journal of Materials Res*earch, 99 (2008), 674.

15. H. Jacobi, "Qualitätsentwicklung bei Sauergasbeständigen Großrohrstählen Vermeidung der Mittenseigerung sowie der Ausscheidung von Mangansulfid un Primärem Niobcarbonitrid" (Habilitation thesis, TU Clausthal, Clausthal-Zellerfeld order No. SE 95 11 357, VDEh 5.4555 B, 1991).

16. H. Jacobi and K. Wünnenberg, "Solidification Structure and Micro-segregation of Unidirectionally Solidified Steels," *Steel Research*, 70 (1999), 362.

17. H. Jacobi, "Investigation of Centreline Segregation and Centreline Porosity in CC-Slabs," *Steel Research*, 74 (2003), 667.

18. H. Tamehiro et al., "Effect of Accelerated Cooling after Controlled Rolling on the Hydrogen Induced Cracking Resistance of Line Pipe Steel," *Transactions of the Iron and Steel Institute of Japan*, 25 (9) (1985), 982-988.

19. C. Bosch et al., "HIC Performance of Heavy Wall Large-diameter Pipes for Sour Service Applications under Fit-for-Service Conditions" (Paper presented at Corrosion 2010, NACE International, Houston, TX, USA, 2010), paper 280.

20. C. Bosch, J-P. Jansen and T. Herrmann, “Fit-for-Purpose HIC Assessment of Large-diameter Pipes for Sour Service Application” (Paper presented at Corrosion 2006, NACE International, Houston, TX, USA, 2006), paper 124.